The Pneumatron is a device based on hardware and software open-sources that allows the measurement of air inside plants, generating high time-resolution estimation of embolism vulnerability. It represents an easy, low-cost, and powerful tool for both laboratory and field measurements.

The Pneumatron: an automated pneumatic apparatus for estimating xylem vulnerability to embolism at high temporal resolution

Luciano Pereira[1,2*†], Paulo R. L. Bittencourt[3,4†], Vinícius S. Pacheco[4], Marcela T. Miranda[1], Ya Zhang[5], Rafael S. Oliveira[4], Peter Groenendijk[4], Eduardo C. Machado[1], Melvin T. Tyree[6], Steven Jansen[5], Lucy Rowland[3] and Rafael V. Ribeiro[2,*†]

[1] Laboratory of Plant Physiology "Coaracy M. Franco", Center R&D in Ecophysiology and Biophysics, Agronomic Institute (IAC), Campinas SP, Brazil.

[2] Laboratory of Crop Physiology, Department of Plant Biology, Institute of Biology, P.O. Box 6109, University of Campinas (UNICAMP), 13083-970, Campinas, SP, Brazil.

[3] College of Life and Environmental Sciences, University of Exeter, Exeter, United Kingdom.

[4] Department of Plant Biology, Institute of Biology, P.O. Box 6109, UNICAMP, 13083-970, Campinas, SP, Brazil.

[5] Institute of Systematic Botany and Ecology, Ulm University, Albert-Einstein-Allee 11, 89081 Ulm, Germany.

[6] College of Chemistry and Life Sciences, Zhejiang Normal University, 688 Yingbin Ave., Jinhua, Zhejiang, 321004, China.

[†] These authors contributed equally to this work.

*Authors for correspondence: biolpereira@gmail.com; rvr@unicamp.br

Funding: São Paulo Research Foundation (FAPESP, Brazil): grants #2017/14075-3 #2018/09834-5, #2018/01847-0, and #2019/07773-1. National Council for Scientific and Technological Development (CNPq, Brazil), grant #401104/2016-8. UK NERC grant NE/N014022/1. Royal Society is Newton International grant NF170370.

Abstract: Xylem vulnerability to embolism represents an important trait to determine species distribution patterns and drought resistance. However, estimating embolism resistance frequently requires time-consuming and ambiguous hydraulic lab measurements. Based on a recently developed pneumatic method, we present and test the "Pneumatron", a device that generates high time-resolution and fully automated vulnerability curves. Embolism resistance is estimated by applying a partial vacuum to extract air from an excised xylem sample, while monitoring the pressure change over time. While the amount of gas extracted is strongly correlated with the percentage loss of xylem conductivity, validation of the Pneumatron was performed by comparison with the optical method for *Eucalyptus camaldulensis* leaves. The Pneumatron improved the precision of the pneumatic method considerably, facilitating the detection of small differences in the percentage of air discharged (PAD < 0.47%). Hence, the Pneumatron can directly measure the 50% PAD without any fitting of vulnerability curves. PAD and embolism frequency based on the optical method were strongly correlated (r^2 = 0.93) for *E. camaldulensis*. By providing an open source platform, the Pneumatron represents an easy, low-cost, and powerful tool for field measurements, which can significantly improve our understanding of plant water relations and the mechanisms behind embolism.

Key-words: pneumatic method, vulnerability curves, cavitation, drought resistance, water transport, plant hydraulics.

Acknowledgments: The authors acknowledge the São Paulo Research Foundation (FAPESP, Brazil) for granted fellowship (L.P. & R.V.R., Grant #2017/14075-3; R.S.O., Grant #2019/07773-1; P.G. #2018/01847-0) and scholarship (M.T.M. & R.V.R., Grant #2018/09834-5). R.V.R., E.C.M, R.S.O. and V.S.P. also acknowledge the fellowships and scholarship granted by CNPq. L.R. also thanks UK NERC for an independent fellowship grant (NE/N014022/1) and P.R.L.B. thanks the Royal Society is Newton International for the fellowship (NF170370). This study was supported by the National Council for Scientific and Technological Development (CNPq, Brazil), Grant #401104/2016-8 (R.V.R.). We acknowledge Sabah Biodiversity Centre for permission to conduct research at the Forest Research Centre, Sepilok, for local collaboration and facilitating access to field sites.

Introduction

Drought-induced embolism of water conducting cells in xylem has been related to tree mortality and loss of primary productivity (Adams *et al.* 2017; Choat *et al.* 2018), with relevance not only for plant ecology but also for agricultural sciences. However, accurately and efficiently measuring xylem embolism is not an easy task, especially in the field, because most methods rely on hydraulic measurements requiring manipulation of xylem tissue that is typically under negative pressure (Jansen, Schuldt & Choat 2015). Conducting hydraulic measurements is far from straightforward because of various reasons, hence, most studies on xylem embolism resistance are at the species level and intra-specific and intra-individual variations are not well understood (but see Pratt, Jacobsen, Ewers & Davis 2007; Lachenbruch & McCulloh 2014; Charrier *et al.* 2016; Rodriguez-Zaccaro *et al.* 2019). Consequently, the current applications of embolism resistance data remain limited. For example, we are far from using it as a trait to select drought tolerant genotypes, to predict how drought may affect trees at the population level and assembly processes for species-rich communities (see Oliveira *et al.* 2018; Barros *et al.* 2019).

The vulnerability curves may be estimated either by directly measuring the loss of conductivity due to embolism formation or by quantifying the number or volume of embolised vessels (Venturas *et al.* 2019). The loss of conductivity is measured directly by using a hydraulic apparatus (Sperry, Donnelly & Tyree 1988) or Cavitron centrifuge (Cochard 2002), while embolism is quantified through 2-D or 3-D images (Brodersen, McElrone, Choat, Matthews & Shackel 2010; Brodribb *et al.* 2016), acoustic emissions (Milburn 1973), or airflow using the pneumatic method (Pereira *et al.* 2016). Although measuring xylem conductivity in intact plants would be desirable, the use of plant segments coupled with a hydraulic apparatus is subject to interferences such as the background flow (Hacke *et al.* 2015; Pereira & Ribeiro 2018), wounding response, introduction of air bubbles (Espino & Schenk 2011), ionic effect (Jansen *et al.* 2011), or potential refilling of embolised conduits (Melcher *et al.* 2012). Besides, the measurements are time-consuming and need a lot of plant material.

We recently presented the pneumatic method as an alternative approach to estimate xylem vulnerability curves for a single branch (Pereira *et al.* 2016; Zhang *et al.* 2018). This

method measures the kinetics of pressure change: by connecting a simple and low-cost apparatus that is composed of a pressure sensor and tubing. The apparatus measures the amount of gas extracted from plant tissue, especially xylem, and is monitored over time, while the plant tissue desiccates. A central assumption of this method is that the amount of air discharged from a particular xylem tissue is related to the amount of embolised conduits. While earlier studies show a striking correlation between the amount of gas extracted in pneumatic experiments and the loss of hydraulic conductivity based on hydraulic measurements for more than 20 species (Pereira *et al.* 2016; Zhang *et al.* 2018), modelling of the gas diffusion kinetics will be needed to fully understand why the amount of gas extracted from xylem is related to embolism. Basic physical laws that underlie pneumatic measurements include Fick's law for diffusion, Henry's law for partitioning of gas concentration between liquid and gas phases at equilibrium, and the ideal gas law. By drawing a partial vacuum in pneumatic experiments, the equilibrium concentration of air in water is changed according to Henry's law. Therefore, gas dissolved in water will diffuse to reach the reduced concentration of air in the partial vacuum of the vessels that are cut open and embolised. Hence, gas extracted with a pneumatic apparatus may include gas from embolised conduits (including both cut-open conduits near the cut end and non-open conduits), intercellular spaces, gas released by parenchyma cells, or gas from air-saturated xylem sap.

One of the major advantages of the pneumatic method is that it relies on bench dehydration to induce embolism, which is not known to cause potential artefacts as reported for air-injection and centrifuge methods (Cochard *et al.* 2013; Yin & Cai 2018; Lamarque *et al.* 2018). Moreover, hundreds or even thousands of gas extraction measurements can be made during the dehydration time as each measurement takes less than 2.5 min. This task is simplified by using an automated pneumatic device. Also, an automated device will likely reduce undesired variation or errors associated with the manual pneumatic measurement procedure. Thus, continuous monitoring of gas diffusion kinetics would remove these errors and substantially improve the accuracy of the vulnerability curves estimated by a pneumatic apparatus.

Here, an automated pneumatic apparatus, the 'Pneumatron', was tested. This device can be programmed to automatically measure the air discharged from a connected plant organ

at 0.5 s intervals with a resolution about 1 ms. It uses a small vacuum pump and a solenoid valve connected to a microcontroller with a pressure sensor and a datalogger. It is possible to connect a stem psychrometer to the same sample to measure water potential simultaneously, which then provides a fully automated approach to construct vulnerability curves. Here, we present: (i) the Pneumatron as a novel approach to estimate xylem embolism, with a comparison of this method either to the hydraulic method in branches (Sperry *et al.* 1988) or to the optical method proposed by Brodribb *et al.* (2016) for leaves; and (ii) the M-Pneumatron, a modified Pneumatron that automatically measures multiple samples at the same time. The Pneumatron and M-Pneumatron allow measurements of gas diffusion kinetics with high temporal resolution both in the lab and in the field, enabling estimates of inter-branch variation to be measured and highlighting its potential as a powerful tool for studying vulnerability to xylem embolism.

Materials and Methods

The Pneumatron - an automated pneumatic apparatus

The Pneumatron follows the same principle as the manual pneumatic method to estimate xylem vulnerability curves (Pereira *et al.* 2016; Zhang *et al.* 2018). In short, a partial vacuum (45 kPa) is applied to the cut base of a branch, with or without removing the bark, and the volume of air extracted (air discharged, AD in μL) is estimated by measuring the pressure increase inside a tube (Fig. 1) of the apparatus after 30 s. The Pneumatron includes (1) a partial vacuum pump to generate sub-atmospheric pressure, (2) a solenoid valve to apply the vacuum to a xylem sample, (3) a pressure transducer to monitor the pressure, and (4) a microcontroller to control the system (i.e. pump, valve and transducer) and to monitor the data (Fig. 1).

We used an ATmega328P microcontroller (Microchip Technology, Chandler Az, USA) assembled in an Arduino Uno prototyping board (Adafruit Industries, New York NY, USA). The Arduino Uno was linked to a data logger shield (Adafruit Industries, New York NY, USA) with a real time clock (DS1307, Maxim Integrated, California, US) and a SD card connector. A 16 bits analogic-digital converter with programmable gain amplifier (ADS1115, Texas Instruments, Dallas TX, USA) was used to read the output pressure of a pressure transducer (PX26-015GV, Omega Engineering, Norwalk CT, USA; manufactured

by Honeywell with part number 26PCCFA6D). This allowed us to have a pressure resolution of ~0.01 kPa. To control the solenoids and vacuum pump, we either used a 2-channels relay module (Ningbo Songle Relay Co., Ltd., Yuyao, Zhejiang, China) or low side N-channel MOSFET transistors (IRLZ44, Vishay Intertech, Pennsylvania, USA) as microcontrolled power switches. We used a vacuum pump (DQB380-FB2, Dyx, Shenzhen, China) to generate vacuum and a three-way mini-solenoid valve (Fa0520F, Dongguan City-Electric Co., Ltd., Dongguan) to control air flow (Fig. 1). The 16 bits analogic-digital converter, SD card, vacuum sensor, real time clock and power switches were installed in a custom-made Arduino Shield, which was designed and developed by the Plant and Environment Technology (Plantem, Campinas SP, Brazil).

Measurements of the amount of air discharged from the plant with the Pneumatron involve a two-step process (Figs. S2 and S3). Firstly, the microcontroller activates a mini-vacuum pump and the mini-solenoid valve. Then, the air pressure inside the tubing connected to the branch decreases to ~40 kPa (absolute), which takes less than one second. The microcontroller then turns off the vacuum pump and the mini-solenoid valve. As a partial vacuum is created inside the tubing in this first second, the air begins to be sucked from the plant tissues and, for this reason, the pressure increases with time. Thus, the volume of air sucked is calculated considering the pressure change from this initial (1 or 2 s)_to the final moment (30 s, see Data analysis section). The Pneumatron records the pressure inside the tubing in a SD memory card every 500 or 1000 ms over 30 s (final pressure). While earlier measurements were based on 150 seconds, we shortened the timing to 30 seconds, which appeared to be sufficient. After this step, the mini-solenoid valve opens to equilibrate the pressure of the plant and discharge tubes with the atmosphere and one measurement is finished. There is a time lag (typically 15 min) for the next programmed measurement and this interval can be adjusted depending on the dehydration speed of the species and the temporal resolution required, although the time interval should be long enough to restore atmospheric pressure inside embolised conduits. The apparatus leakage was lower than 12 and 22.6 μL during the discharge curve in leaves and branches, respectively, which was lower than the minimum AD values measured from leaves (> 19 μL) and branches (> 100 μL).

A second version of the Pneumatron, the Multiple Pneumatron or M-Pneumatron, was built to take automated measurements of ten branches at the same time by using ten

normally closed solenoid valves (DSF2-A, Dyx, Shenzhen, China). Herein, measurements of the air discharged were taken every 15 min with the Pneumatron and every 30 min with the M-Pneumatron (time required to measure all ten branches). See the Supporting Information for the general setup of the Pneumatron (Fig. S1) and the M-Pneumatron (Fig. S2), the scheme of the electronic connections (Fig. S3), the Arduino programming scheme (Fig. S4), and the scripts (Methods S1).

Plant material

Measurements with the Pneumatron were taken in June 2018 on four orange trees (*Citrus sinensis* L. Osbeck grafted on *Citrus limonia* Osbeck), which were about 1 m tall and had a stem diameter of ca. 15 mm. This species was selected because plenty of plant material was available, while earlier experiments had shown that considerable variation occurred in the vulnerability curves at an intraspecific and intra-plant level. The plants were grown in pots of 4.5 L, containing *Pinus* bark as substrate, and kept under greenhouse conditions at Campinas (22°54'23"S, 47°3'42"O, São Paulo State, Brazil), where air temperature varied from 18 to 42°C. Between February and March of 2019 three mature leaves of a *Eucalyptus camaldulensis* Dehnh. tree (about 5 m tall and growing in Campinas) were also used for the estimation of leaf embolism.

We compared measurements with Pneumatron and hydraulic apparatus in branches of *Eucalyptus camaldulensis* and *Schinus terebinthifolius* trees. Previously, we used the bench dehydration method and the hydraulic apparatus to estimate the vulnerability curves (Pereira *et al.* 2016). These curves were compared with the Pneumatron measurements, using branches of the same *S. terebinthifolius* tree and branches of an *E. camaldulensis* tree cultivated from the seedlings used in the previous report (Pereira *et al.* 2016).

For the M-Pneumatron measurements, we collected sun-exposed branches from five *Shorea multiflora* (Burck) Sym. (Dipterocarpaceae) mature trees at the Sepilok Forest Reserve, in Sandakan, Malaysia (5°52'48"N, 117°56'42"E). For each tree, we measured two terminal branches, with a diameter close to 1 cm and length of 60 to 100 cm.

The above-ground tissues of citrus trees and *S. multiflora* were collected early in the morning, immediately bagged in black plastic bags to avoid dehydration and transported to

the laboratory. Then, the bases of the branches were connected to sections of a silicone tube using plastic clamps (RZ-06832-02, Cole-Parmer, Vernon Hills IL, USA), without removing the bark tissue. We used adapter luers (EW-30800-06, Cole-Parmer, Vernon Hills IL, USA) and PVC tubing (EW-30600-62, Cole-Parmer, Vernon Hills IL, USA) to connect the silicone tube to the Pneumatron. In addition, we used polyvinyl acetate glue to avoid leakages in the connection with the branch. We used this glue to seal any leakages between the tubes and the bark, as well as to seal cut leaves and small branches present near to the connection. The volume of the discharge tube (V_r) was 2.77 mL for citrus and 8 mL for *S. multiflora*.

Leaves of *E. camaldulensis* were also collected early in the morning and its petioles were cut under distilled water. The petioles were kept underwater while the leaf blades were fixed on the scanner for taking measurements with the optical method (see the section "Embolism measurements of leaf xylem"). Then, the petioles were connected to a silicone ring using the same clamps and adapters described above and we also used parafilm and polyvinyl acetate glue to avoid gas diffusion leakages. We used a small discharge tube V_r 0.68 mL) to increase the Pneumatron resolution (see "Theoretical precision of the Pneumatron" section) as the volume of petiole and leaf veins is considerably smaller than the branches.

Xylem water potential

For the Pneumatron measurements, the stem water potential was automatically and simultaneously measured with the air discharged, using a stem psychrometer (ICT International, Armidale NSW, Australia). The stem psychrometer was installed at a distal part of branches for *C. sinensis* and set up for measurements every 15 or 30 min to test the best interval for a better vulnerability curve estimation. We also tested if using a partially bagged branch would improve the resolution of the curve by slowing dehydration. When taking measurements of *E. camaldulensis* and *S. terebinthifolius* branches or using the M-Pneumatron, the xylem water potential was measured at intervals of 1 to 5 h, using a pressure chamber (PMS 1000, PMS Instruments Co., Albany OR, USA). The ten branches were bagged up for at least 30 min to obtain a leaf and xylem water potential equilibrium prior to measurements with a pressure chamber. The xylem water potential between each interval of

measurements was estimated assuming a linear decrease of xylem water potential during dehydration. Using the water potential data from the psychrometer measurements, we also correlated the estimated (based on linear variation) and measured water potential during dehydration, considering intervals from 1 to 5 hours between measurements.

Embolism measurements of leaf xylem

We used the optical method proposed by Brodribb *et al.* (2016) to estimate vein embolism, using a scanner (Model 12000XL, Epson America Inc., San Jose CA, USA) while the Pneumatron was connected to the petiole of the same leaf. Three leaves of the same *Eucalyptus camaldulensis* tree were used for this experiment. The scanner was programmed to take an image every 15 min and the Pneumatron was programed to measure AD at the same time interval for about 30 hours, which was the time needed for the leaves to become completely dehydrated. The images were processed according to instructions of the open source project OpenSourceOV (http://www.opensourceov.org/). The images were cut and aligned using the OSOV toolbox as small leaf movement was noticed inside the scanner during dehydration. Then, the formation of vein embolism over time was estimated for each leaf from at least three subregions of each leaf blade.

Data analysis

As described in Pereira *et al.* (2016), the increase in moles of air discharged in the tubes (Δn, mol) was calculated according to the ideal gas law using the initial (P_i, in kPa) and final (P_f) pressure measured:

$$\Delta n = n_f - n_i = P_f V_r / RT - P_i V_r / RT \quad (1)$$

where n_i (mol) is the initial number of moles of air and n_f (mol) is the final number after a predetermined time. R is the gas constant (8.314 kPa L mol^{-1} K^{-1}), T is the room temperature (20º C = 293.15 K), and V_r is the discharging tube volume (L). The equivalent volume of air (Air Discharged, AD in µL) at atmospheric pressure (P_{atm}, 98 kPa) was calculated as follows:

$$AD = (\Delta nRT / P_{atm})*10^6 \quad (2)$$

The minimum (AD_{min}, when the branch is well-hydrated) and the maximum (AD_{max}, when AD stopped increasing even with a decreasing water potential) AD measurements were used to calculate the Percentage of Air Discharged (PAD, %) as:

$$PAD = 100*(AD - AD_{min}) / (AD_{max} - AD_{min}) \quad (3)$$

The PAD values were fitted to the following logistic function (Pammenter & Vander Willigen 1998):

$$PAD = 100/(1 + \exp((S/25)(\Psi_x - \Psi_{50}))) \quad (4)$$

where Ψ_x is the water potential measured for a given PAD, Ψ_{50} is the Ψ_x when PAD equals 50%, and S (%PAD MPa^{-1}) is the slope of the curve.

The data were processed in the programming environment R with basic statistical packages (R Core Team 2013).

Theoretical precision of the Pneumatron

The theoretical resolution of the Pneumatron was estimated considering the linearity of the pressure sensor described by the manufacturer (0.25% of the full scale) from zero to 100 kPa. Then, 0.25 kPa was considered as the difference between P_i and P_f to estimate the AD error range, considering a given discharge tube volume (V_r). Then, we estimated the AD error while varying V_r, from 0.5 to 4 mL, which represented volumes typically used in our experiments for several species. The possible AD_{max} measured was calculated considering 50 kPa of difference between P_i and P_f for the same range of discharge tube volume (from 0.5 to 4 mL). The difference of 50 kPa turns the pressure inside the tubbing to almost atmospheric at the moment of P_f, and in this case, gas would no longer be sucked from plant tissues.

306

307 **Results**

308

309 *Air discharge curves*

310

311 The Pneumatron measured air discharged (AD) of the samples with high temporal
312 resolution (Fig. 2). The amount of air discharged was initially low and progressively
313 increased during dehydration of all *C. sinensis* samples, reaching a plateau after some time.
314 On the other hand, xylem water potential continued decreasing even after the AD plateau had
315 been reached. The high temporal resolution showing a stable AD_{max} allowed us to estimate
316 with confidence the PAD. Based on PAD estimated for each branch, we found both the water
317 potential leading to 50% reduction in PAD, i.e. Ψ_{50}, as well as the dehydration time for
318 reaching Ψ_{50} in each sample (-2.35 MPa, 3.1 h; -1.86 MPa, 3.8 h; -1.65 MPa, 2 h; -2.32 MPa,
319 10.9 h, for samples of *Citrus sinensis* 1, 2, 3 and 4, respectively; Fig. 3).
320 Monitoring pressure values every 500 ms within each AD measurement revealed that
321 the shape of AD curves changed during dehydration, following decreases in xylem water
322 potential (Fig. 4a). While the final pressure (P_f) changed significantly during the branch
323 dehydration (Fig. 4c), the initial pressure (P_i) did not present relevant changes (Fig. 4b).
324 The theoretical resolution of the Pneumatron, or error range, was correlated to the
325 volume of the discharge tube used in the pneumatic apparatus. Such AD error varied from
326 about 1 to 10 μL and is given by $AD_{error} = 2.551*V_r$ (Fig. S5). In the same way, AD_{max} may
327 vary from about 200 to 2000 μL, being correlated to V_r as: $AD_{max} = 510.2*V_r$ (Fig. S5). The
328 actual average resolution of the Pneumatron was 0.47% when considering the loss of
329 conductance in *C. sinensis* and assuming PAD = PLC (percentage loss of conductivity). This
330 resolution was obtained with 15 min of interval between measurements and under slow
331 dehydration by bagging branches partially (Fig. 3d).

332

333 *Automated vulnerability curves with the M-Pneumatron*

334

335 The AD curves of the *S. multiflora* samples measured with the M-Pneumatron
336 showed non-embolised (lower plateaus) or fully embolised (upper plateaus) branches (Fig.

5). The strategy of sampling xylem water potential at every 3 to 5 h interval and interpolating the data allowed us to produce high resolution vulnerability curves (Fig. 6). In fact, the quality of interpolated water potential data using different time intervals (1, 3 and 5 h) was evaluated in *C. sinensis* by comparing the interpolated data with the actual measured data. Although the error increased with increasing time interval, it remained low, and the interpolated xylem water potential data had a high correlation with the measured data (Fig. S6). For all *C. sinensis* samples the coefficient of determination of the predicted values (r^2) was higher than 0.99 for time intervals from 1 to 4 h, and higher than 0.97 for 5 h of interval.

Comparing the hydraulic apparatus and the Pneumatron measurements

The 50% loss of conductivity and 50% of air discharged were strongly correlated for *S. terebinthifolius* and slightly different for *E. camaldulensis*, although the curves estimated with the hydraulic method presented more significant error due to data scattering (Fig. 7). For *S. terebinthifolius,* the mean Ψ_{50} estimated with the Pneumatron was -3.3 ± 0.1 MPa and -3.1 ± 0.2 MPa when estimated with the hydraulic apparatus. For *E. camaldulensis*, the Ψ_{50} estimated was -4.7 ± 0.1 MPa with the Pneumatron and -4.1 ± 0.4 MPa with the hydraulic apparatus.

Comparing the optical and pneumatic methods to estimate leaf embolism formation

Leaf embolism formation evaluated with the optical method (as vein embolism) and with the Pneumatron (as air discharge) was similar and data from both methods were highly correlated over time ($r^2 > 0.93$, $P < 0.0001$, Fig. 8). However, measurements taken with the Pneumatron during the first hours of dehydration (from 60 to 285 min) were unstable, with high AD values measured before reaching the AD_{min} (Fig. S7). As there was no vein embolism formation during this time, we did not consider those initial AD values to calculate the PAD. Interestingly, the period of instability corresponded to about one third of the total time required to see the first event of vein embolism occurred, regardless whether the dehydration was slow of fast.

Discussion

The development of an automated Pneumatron instrument provides an important step forward in quantifying gas diffusion, offering a higher temporal resolution and higher accuracy in recording air discharge volumes than the manual approach. Moreover, our results show that the amount of gas extracted from leaves of *E. camaldulensis* corresponded very well with the amount of embolism detected in leaf veins using the optical method (Brodribb *et al.* 2016), which provides additional confirmation that PAD is related to xylem embolism. As such, combining the Pneumatron with stem psychrometers offers a novel and fully automated approach to obtain detailed vulnerability curves both in the lab and under field conditions, as its low power consumption allows using the Pneumatron for more than three days on 12V 70 Ah batteries. Also, the Pneumatron allows for multiple measurements of different samples or plant organs (e.g., roots, stems, leaves) and comparisons at individual level. The capacity to record with precision the time when a given level of embolism was reached facilitates experimentation of drivers of embolism on desiccating plants. The limitations of the methods and our current interpretation of changes in gas diffusion of xylem tissue during dehydration deserve further studies and they should be considered when discussing results. Nonetheless, the high-resolution measurements of the Pneumatron open up new possibilities for a wide range of scientific uses, making measurements of embolism resistance relatively easy, fast and feasible.

The Pneumatron allowed the estimation of high time-resolution air discharge and data-point resolution of 0.47% PAD. This high resolution enables inter-branch comparisons (Figs. 3 and 5) and allows for almost a direct measuring of the vulnerability traits (e.g. Ψ_{50} and Ψ_{88}), avoiding uncertainty associated with fitted curves. If branch dehydration is slow and the interval between AD measurements is short enough, the Pneumatron can directly measure the 50% PAD (see differences among fast and slow dehydration and 15 and 30 min of interval for AD measurements in Fig. 2, and the respective vulnerability curves in Fig. 3).

Despite the similarity between vulnerability curves estimated by the pneumatic and hydraulic methods (Pereira *et al.* 2016; Zhang *et al.* 2018), a difference of a few seconds between measurements of air discharge and any delay in opening and closing the three-way valves are sources of error when using the manual pneumatic method. These issues are solved

with the Pneumatron, which uses a microcontroller with a speed of 16 MHz, saving the pressure data every 0.5 s and controlling the vacuum pump and valves with a precision of microseconds. Therefore, the time between consecutive AD measurements is practically the same and the measurements of P_i *and* P_f are much more precise than the manual approach, which requires the operator to write down the pressure values.

The AD curves obtained with the Pneumatron showed a typical increase in the amount of air discharged from branches during dehydration, which reaches a plateau while water potential continues to decrease (Figs. 2 and 6). This further corroborates that AD measurements are reflecting embolism (Pereira *et al.* 2016; Zhang *et al.* 2018) instead of shrinkage of xylem tissue. As shrinkage would be proportional to stem water potential, a continuous increase of AD during dehydration would be expected – without any apparent plateau, which was not found here. Also, the initial AD when the plant tissue is hydrated, should represent gas from non-xylem tissues and from open vessels that are quickly embolised when the plant tissue is cut. Thus, the interference of the non-xylem gas should be minimal, as we subtract the initial AD to calculate the PAD.

The vulnerability curves obtained with the M-Pneumatron and estimation of xylem water potential between AD measurements allowed us to easily measure embolism resistance in several samples simultaneously (Fig. 5). Our analyses of interpolated xylem water potential using the *C. sinensis* data set (Fig. S6) suggests that the time intervals for interpolation should be below 5 h for estimating this plant trait with high accuracy. In general, higher errors were found under not very negative water potential values, when fast changes in water potential are expected during the first stages of desiccation (Fig. S6). Therefore, xylem water potential should be measured more frequently during the first hours of desiccation or for fast desiccating plants.

Similarly to the optical method (Brodribb *et al.* 2016), microtomography (Brodersen *et al.* 2010), and acoustic emissions approach (Milburn 1973; Vergeynst, Dierick, Bogaerts, Cnudde & Steppe 2014), the pneumatic method estimates embolism instead of the percentage loss of conductivity. However, previous comparisons showed a good agreement between the estimated vulnerability curves when using the pneumatic method and the hydraulic apparatus (Pereira *et al.* 2016; Zhang *et al.* 2018) or Cavitron (Zhang *et al.* 2018). In the same way, the curves estimated with the Pneumatron showed a strong agreement with hydraulic

measurements for *S. terenbithifolius* branches, although slight differences for *E. camaldulensis* branches were found (Fig. 7). The difference for *E. camaldulensis* may be due to (i) the significant error of the curve estimated from the data measured using the hydraulic method and (ii) due to differences of plant age when comparing plant material used in each method. Nevertheless, the curves estimated with the Pneumatron presented a much smaller data scattering than with the hydraulic method.

In short, the high temporal resolution, fully automated approach, low-cost, and simple data analyses represent the main advantages of the Pneumatron compared to other available methods. Also, for the pneumatic method, embolism is induced using the bench dehydration technique, which is also used in the imaging and acoustic emissions methods. Using the bench dehydration avoids embolism overestimation due to artefacts, as described for the centrifuge (the open vessel artefact) and double-ended chamber (effervescence artefact) methods (Yin & Cai 2018).

Comparison of the pneumatic and optical method

It is possible to obtain high-resolution vulnerability curves using the optical method for leaves (Brodribb *et al.* 2016), and our results demonstrate a strong correlation of vein embolism and PAD for petioles of *E. camaldulensis* (Fig. 8). The main advantage of the Pneumatron is the ease of connection with the petiole and the simple and fast data analysis. Hundreds of datapoints represent only few megabytes of a text file, and the vulnerability curves are easily calculated in an Excel spreadsheet. Although the Pneumatron is a promising tool for measuring leaf embolism, further research is needed to reveal if it is an applicable device for comparing species with varying leaf morphology. For example, small leaves may have few microliters of air in their veins when totally embolised and this quantity may be undetectable by the Pneumatron described here. Since the internal volume of the solenoid valve and connections determine V_r, these components must be adapted to detect small amounts of gas extracted from leaf veins. It is currently unclear whether leaf morphology and conduit collapse in leaf veins affect gas extraction (Zhang, Rockwell, Graham, Alexander & Holbrook 2016), which would make the pneumatic method problematic for some species.

Although a stable AD_{max} had been measured in fully dehydrated leaves of *E. camaldulensis*, the initial AD measurements were surprisingly high and decreased in one or two hours before reaching its minimum (AD_{min}). The stable AD_{min} that was reached was considered as reference point for PAD calculations (see unstable datapoints in the Fig. S7). Since we have not observed such variable AD measurements when working with stems, the high AD values after connecting the leaf to the Pneumatron may be a consequence of leakages or even air spaces inside leaves from non-xylem tissue that shrink after slight dehydration. Compared to stem samples that have been debarked and typically show a very small or no pith tissue at all, the amount of non-xylem tissue is most likely much higher in leaf petioles than in stem samples. Interestingly, this instability occurred long before vein embolism started, even in a situation of fast (Fig. 8a and b) or slow dehydration (Fig. 8c). Application of the Pneumatron on leaves with a variable leaf morphology and anatomy would be useful to fully understand these high initial AD values. Moreover, it might be useful to keep leaves in a plastic bag until AD values become stable, while avoiding fast dehydration and embolism. As the Pneumatron can detect small amounts of air from leaves, additional care is needed to avoid leakages in the petiole connection, using parafilm, glue, and a tight clamp.

Pneumatron sensitivity

The sensitivity of the pneumatic apparatus is directly related to the volume of the discharged air in vacuum tubes to estimate the air volume inside plant tissues (Pereira *et al.* 2016), i.e., a small air discharge volume from a leaf or petiole can be measured more precisely if a small discharge tube (V_r) is used. Thus, the AD measurement can be improved if the discharge vacuum volume is taken into account. An estimation of the AD error is shown in Fig. S5, where we considered the linearity of the sensor, which was 0.25% of the full scale according to the manufacturer. In addition, to avoid that the discharge vacuum tubes reach atmospheric pressure and interrupt the air suction from branches, we arbitrarily considered a limit of 90 kPa as a maximum absolute pressure required for an operational Pneumatron. This procedure causes a limitation of the maximum volume of air that can be discharged (Fig. S5, secondary y-axis), which must be considered and depends on the airflow volume that is

extracted from samples. As the latter volume varies among plant species, the airflow volume cannot be predicted from the sample's size (Pereira *et al.*, 2016). Therefore, the volume of the discharge tube has to be tested and defined prior to measurements: the maximum airflow volume should be estimated from a completely dehydrated branch, and the volume of the discharge tube volume should be chosen considering AD_{max}, i.e., discharge tube volume = $AD_{max}/510.2$ (Fig. S5). Alternatively, increasing V_r when pressure is higher than 90 kPa can allow for working with plants that have a high AD range during dehydration.

Conclusion

Embolism vulnerability curves were produced with high-resolution data using the Pneumatron, allowing intra-specific and inter-organ comparison. The automation of the pneumatic method improved the measurement precision compared with the manual pneumatic method. Measurements taken with the Pneumatron, the optical method and the hydraulic method were well correlated. In addition, we were able to easily and simultaneously measure embolism of several samples with the M-Pneumatron. As the Pneumatron is based on an open-source platform, it is a low-cost instrument that can speed up our understanding about plant-water relations. This will increase our understanding of the mechanisms underlying vulnerability to embolism and enables for better predictions of plant performance in an environment where water-availability – a key driver of plant growth and development – is changing.

References

Adams H.D., Zeppel M.J.B., Anderegg W.R.L., Hartmann H., Landhäusser S.M., Tissue D.T., … McDowell N.G. (2017) A multi-species synthesis of physiological mechanisms in drought-induced tree mortality. *Nature Ecology & Evolution* **1**, 1285–1291.

Barros F. V., Bittencourt P.R.L., Brum M., Restrepo-Coupe N., Pereira L., Teodoro G.S., … Oliveira R.S. (2019) Hydraulic traits explain differential responses of Amazonian forests to the 2015 El Nino-induced drought. *New Phytologist*, nph.15909.

522 Brodersen C.R., McElrone A.J., Choat B., Matthews M.A. & Shackel K.A. (2010) The
523 Dynamics of Embolism Repair in Xylem: In Vivo Visualizations Using High-
524 Resolution Computed Tomography. *Plant Physiology* **154**, 1088–1095.
525 Brodribb T.J., Skelton R.P., Mcadam S.A.M., Bienaimé D., Lucani C.J. & Marmottant P.
526 (2016) Visual quantification of embolism reveals leaf vulnerability to hydraulic
527 failure. *New Phytologist* **209**, 1403–1409.
528 Charrier G., Torres-Ruiz J.M., Badel E., Burlett R., Choat B., Cochard H., … Delzon S.
529 (2016) Evidence for Hydraulic Vulnerability Segmentation and Lack of Xylem
530 Refilling under Tension. *Plant Physiology* **172**, 1657–1668.
531 Choat B., Brodribb T.J., Brodersen C.R., Duursma R.A., López R. & Medlyn B.E. (2018)
532 Triggers of tree mortality under drought. *Nature* **558**, 531–539.
533 Cochard H. (2002) A technique for measuring xylem hydraulic conductance under high
534 negative pressures. *Plant, Cell and Environment* **25**, 815–819.
535 Cochard H., Badel E., Herbette S., Delzon S., Choat B. & Jansen S. (2013) Methods for
536 measuring plant vulnerability to cavitation: a critical review. *Journal of Experimental*
537 *Botany* **64**, 4779–4791.
538 Espino S. & Schenk H.J. (2011) Mind the bubbles: achieving stable measurements of
539 maximum hydraulic conductivity through woody plant samples. *Journal of*
540 *Experimental Botany* **62**, 1119–1132.
541 Hacke U.G., Venturas M.D., MacKinnon E.D., Jacobsen A.L., Sperry J.S. & Pratt R.B.
542 (2015) The standard centrifuge method accurately measures vulnerability curves of
543 long-vesselled olive stems. *New Phytologist* **205**, 116–127.
544 Jansen S., Gortan E., Lens F., Lo Gullo M.A., Salleo S., Scholz A., … Nardini A. (2011)
545 Do quantitative vessel and pit characters account for ion-mediated changes in the
546 hydraulic conductance of angiosperm xylem? *New Phytologist* **189**, 218–228.
547 Jansen S., Schuldt B. & Choat B. (2015) Current controversies and challenges in applying
548 plant hydraulic techniques. *New Phytologist* **205**, 961–964.
549 Lachenbruch B. & McCulloh K.A. (2014) Traits, properties, and performance: how woody
550 plants combine hydraulic and mechanical functions in a cell, tissue, or whole plant.
551 *New Phytologist* **204**, 747–764.
552 Lamarque L.J., Corso D., Torres-Ruiz J.M., Badel E., Brodribb T.J., Burlett R., … Delzon

S. (2018) An inconvenient truth about xylem resistance to embolism in the model species for refilling Laurus nobilis L. *Annals of Forest Science* **75**, 88.

Melcher P.J., Holbrook N.M., Burns M.J., Zwieniecki M.A., Cobb A.R., Brodribb T.J., … Sack L. (2012) Measurements of stem xylem hydraulic conductivity in the laboratory and field. *Methods in Ecology and Evolution* **3**, 685–694.

Milburn J.A. (1973) Cavitation in Ricinus by acoustic detection: Induction in excised leaves by various factors. *Planta* **110**, 253–265.

Oliveira R.S., Costa F.R.C., van Baalen E., de Jonge A., Bittencourt P.R., Almanza Y., … Poorter L. (2019) Embolism resistance drives the distribution of Amazonian rainforest tree species along hydro-topographic gradients. *New Phytologist* **221**, 1457–1465.

Pammenter N.W. & Vander Willigen C. (1998) A mathematical and statistical analysis of the curves illustrating vulnerability of xylem to cavitation. *Tree physiology* **18**, 589–593.

Pereira L., Bittencourt P.R.L., Oliveira R.S., Junior M.B.M., Barros F.V., Ribeiro R.V. & Mazzafera P. (2016) Plant pneumatics: stem air flow is related to embolism - new perspectives on methods in plant hydraulics. *New Phytologist* **211**, 357–370.

Pereira L. & Ribeiro R.V. (2018) Radial stem flow and its importance when measuring xylem hydraulic conductance. *Theoretical and Experimental Plant Physiology* **30**, 71–75.

Pratt R.B., Jacobsen A.L., Ewers F.W. & Davis S.D. (2007) Relationships among xylem transport, biomechanics and storage in stems and roots of nine Rhamnaceae species of the California chaparral. *New Phytologist* **174**, 787–798.

R Core Team (2013) R: A language and environment for statistical computing.

Rodriguez-Zaccaro F.D., Valdovinos-Ayala J., Percolla M.I., Venturas M.D., Pratt R.B. & Jacobsen A.L. (2019) Wood structure and function change with maturity: Age of the vascular cambium is associated with xylem changes in current-year growth. *Plant, Cell & Environment* **42**, 1816–1831.

Sperry J.S., Donnelly J.R. & Tyree M.T. (1988) A method for measuring hydraulic conductivity and embolisms in xylem. *Plant, Cell & Environment* **11**, 25–40.

Venturas M.D., Pratt R.B., Jacobsen A.L., Castro V., Fickle J.C. & Hacke U.G. (2019) Direct comparison of four methods to construct xylem vulnerability curves:

differences among techniques are linked to vessel network characteristics. *Plant, Cell & Environment*, 1–15.

Vergeynst L.L., Dierick M., Bogaerts J.A.N., Cnudde V. & Steppe K. (2014) Cavitation: a blessing in disguise? New method to establish vulnerability curves and assess hydraulic capacitance of woody tissues. *Tree Physiology* **35**, 400–409.

Yin P. & Cai J. (2018) New possible mechanisms of embolism formation when measuring vulnerability curves by air injection in a pressure sleeve. *Plant, Cell & Environment* **41**, 1361–1368.

Zhang Y.-J., Rockwell F.E., Graham A.C., Alexander T. & Holbrook N.M. (2016) Reversible Leaf Xylem Collapse: A Potential "Circuit Breaker" against Cavitation. *Plant Physiology* **172**, 2261–2274.

Zhang Y., Lamarque L.J., Torres-Ruiz J.M., Schuldt B., Karimi Z., Li S., … Jansen S. (2018) Testing the plant pneumatic method to estimate xylem embolism resistance in stems of temperate trees. *Tree Physiology* **38**, 1016–1025.

Figures

Fig. 1 – Automated pneumatic apparatus scheme for measurements of gas diffusion kinetics of plant, and especially xylem tissue. The apparatus was composed by a microcontroller (Arduino Uno), a data logger shield (not shown; coupled up Arduino), an analogical-to-digital converter (ADS1115), a relay module (power switches), a mini-vacuum pump, solenoid valves and a pressure transducer. The plant tissue is connected to the apparatus by using adapter Luers (Cole-Parmer, catalog numbers: EW-30800-06 and EW-30800-24), silicone tubes (different diameters), and rigid tubes (Cole-Parmer, catalog number: EW-30600-62), depending on the desired tubing volume (V_r, see Materials and Methods section). Alternative parts and assembling, with an additional solenoid for atmosphere connection and MOSFET transistors as power switches, are shown in the Supporting Information. The device is connected here to a stem sample.

Fig. 2 – Automated measurements of air discharged (AD, red) and xylem water potential (blue) of branches of four *Citrus sinensis* individuals during bench dehydration. Air discharged was measured with the Pneumatron and xylem water potential with a stem psychrometer. In (a) the AD and water potential were measured every 30 min and in (b), (c), and (d) every 15 min. The branch (d) was partially bagged to allow a slow dehydration. Note air discharged reaches a plateau, indicating fully embolised xylem, while water potential shows a continuous decreasing trend.

Fig. 3 – Percentage of air discharged as a function of xylem water potential for four *Citrus sinensis* individuals (see Fig. 2). Triangle and dashed lines indicate the Ψ_{50}. The "t" in the lower-left part of each panel is the approximate desiccation time when plants reached the Ψ_{50}. The black line marks the sigmoidal fit.

Fig. 4 – Example of air discharge curves during 30 s (a) and the relationship between the xylem water potential and initial (P_i, b) and final (P_f, c) pressures in all 186 air discharged curves (c) from a dehydrating branch of *Citrus sinensis*. The final pressure (P_f) at 30 s increases with decreasing xylem water potential during branch dehydration (c).

631

632 **Fig. 5** – Automated air discharged curves measured simultaneously with the M-Pneumatron,
633 during dehydration for ten branches of five *Shorea multiflora* individuals. Curves with
634 different colors indicate different individuals and different symbols with the same color
635 indicate different branches from a given individual.

636

637 **Fig. 6** – Air discharged (red) and xylem water potential (blue) during desiccation (a) and the
638 percentage of air discharged as a function of xylem water potential (b) of one *Shorea*
639 *multiflora* branch. Large, closed, blue circles are measured xylem water potential, while
640 small, open, blue circles are estimated xylem water potentials. In (b), "t" is the approximate
641 desiccation time when plants reached the Ψ_{50}, which was marked with a black triangle. The
642 black line marks the sigmoidal fit.

643

644 **Fig. 7** – Vulnerability curves of *Schinus terenbithifolius* and *Eucalyptus camaldulensis*
645 branches, estimated using a hydraulic apparatus (in red, percentage loss of conductivity –
646 PLC, and the respective Ψ_{50} values in red) and the Pneumatron (in blue, percentage of air
647 discharged – PAD). Black lines represent the sigmoidal adjust, considering all branches
648 measured with the Pneumatron (N=4, and the respective Ψ_{50} values in black) and the blue
649 Ψ_{50} values are the averages considering the estimation for each branch.

650

651 **Fig. 8** – Vein embolism (blue points, %) and percentage of air discharged (red points, PAD,
652 %) over time in three leaves of *Eucalyptus camaldulensis*. Note in (a) and (b) the leaf
653 dehydration was faster than in (c). The r^2 indicate the correlation between the measurements
654 using both methods over time.

655

656 **Supporting Information**

657

658 **Fig. S1** General aspect of Pneumatron.
659 **Fig. S2** General aspect of M-Pneumatron.
660 **Fig. S3** Scheme of electronic connections.
661 **Fig. S4** Scheme of programming for Pneumatron.

662 **Fig. S5** Estimation of the air discharged error and maximum AD.

663 **Fig. S6** Relationship between measured and predicted xylem water potential.

664 **Fig. S7** Initial unstable AD datapoints in the leaf measurements.

665

666 **Methods S1** Arduino Script for Pneumatron.

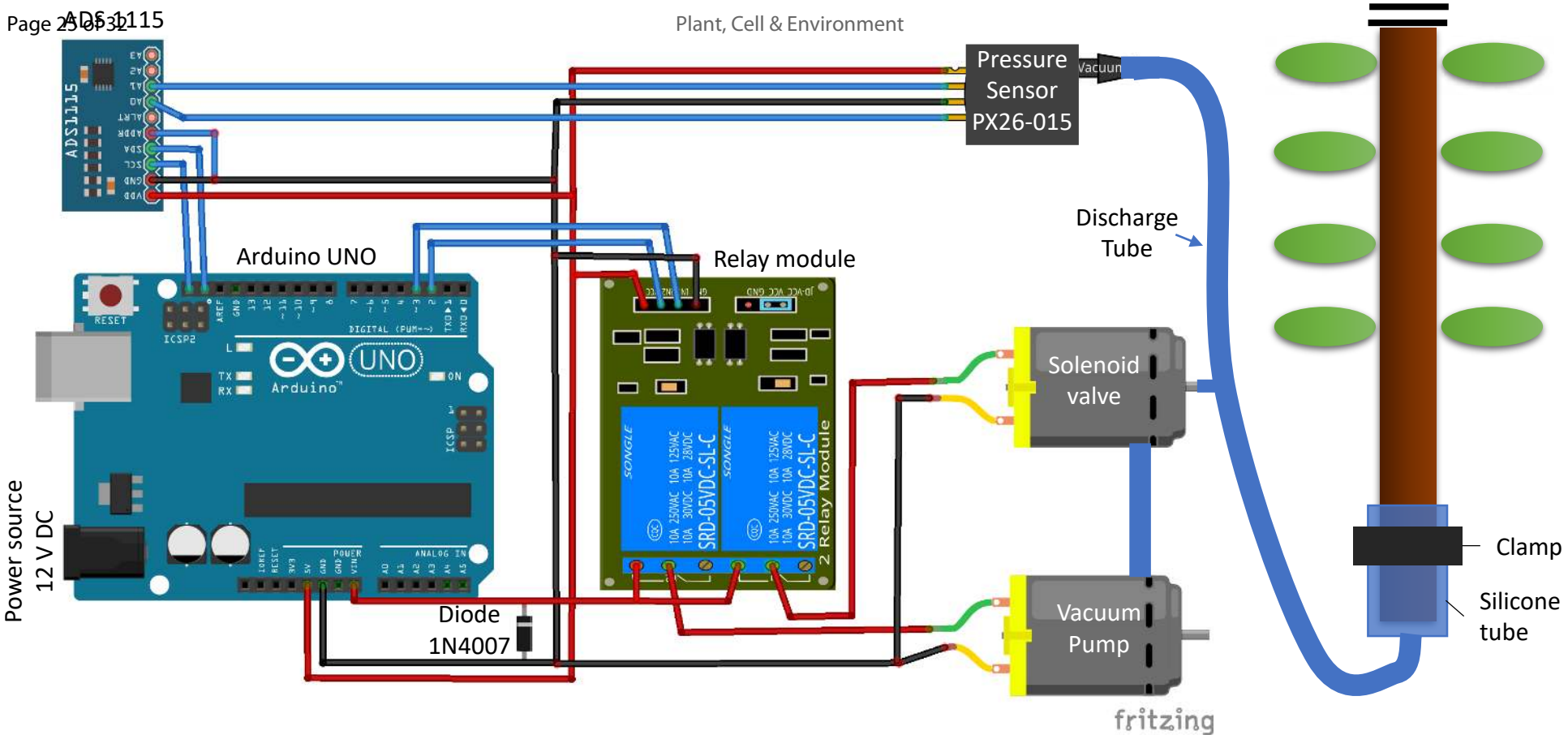
ADS1115
Pressure Sensor PX26-015
Vacuum
Discharge Tube
Arduino UNO
Relay module
Solenoid valve
Vacuum Pump
Clamp
Silicone tube
Power source 12 V DC
Diode 1N4007
2 Relay Module
SRD-05VDC-SL-C
fritzing

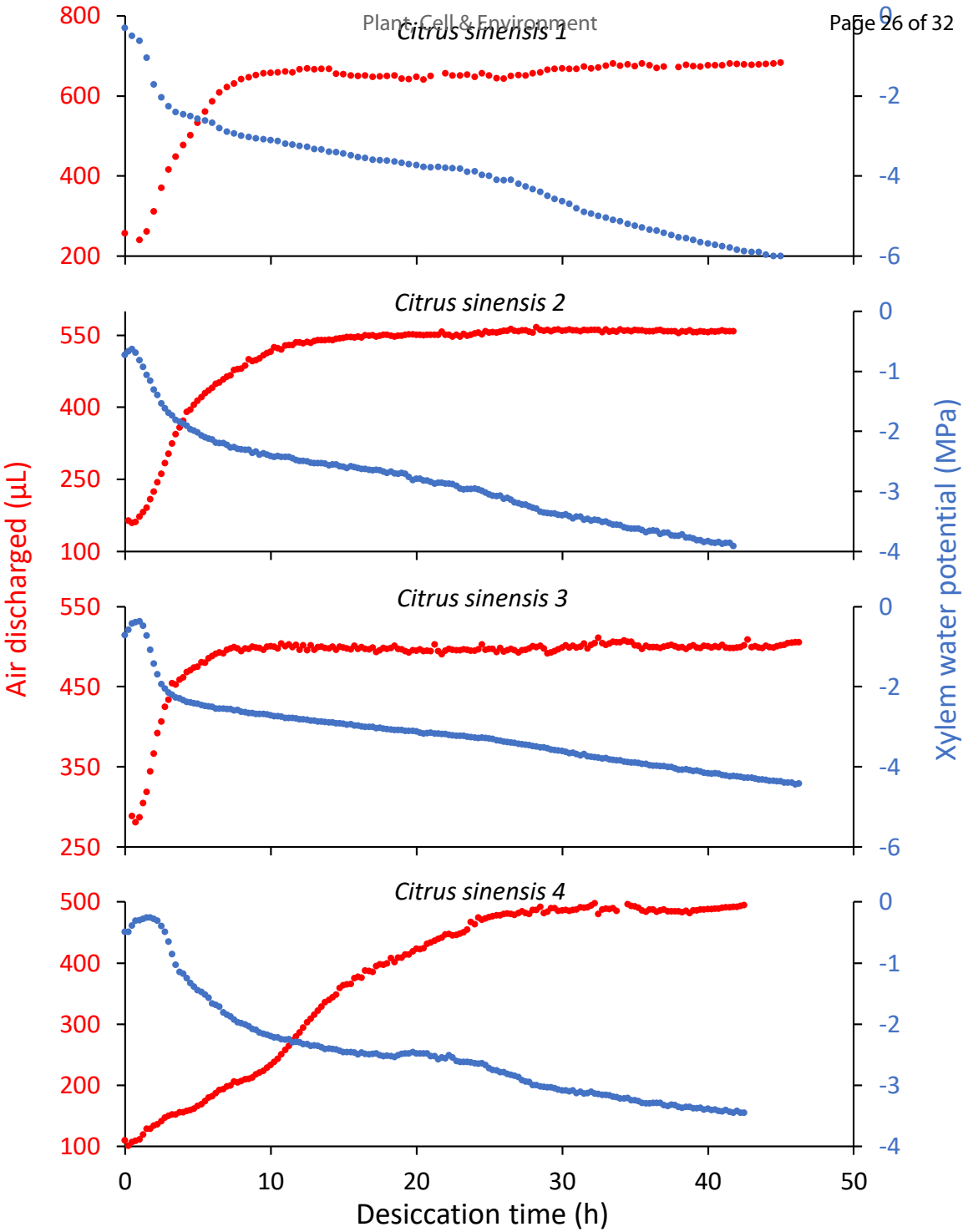
Citrus sinensis 1
Citrus sinensis 2
Citrus sinensis 3
Citrus sinensis 4
Air discharged (µL)
Xylem water potential (MPa)
Desiccation time (h)
800
600
400
200
550
400
250
100
550
450
350
250
500
400
300
200
100
0
-2
-4
-6
0
-1
-2
-3
-4
0
-2
-4
-6
0
-1
-2
-3
-4
0
10
20
30
40
50

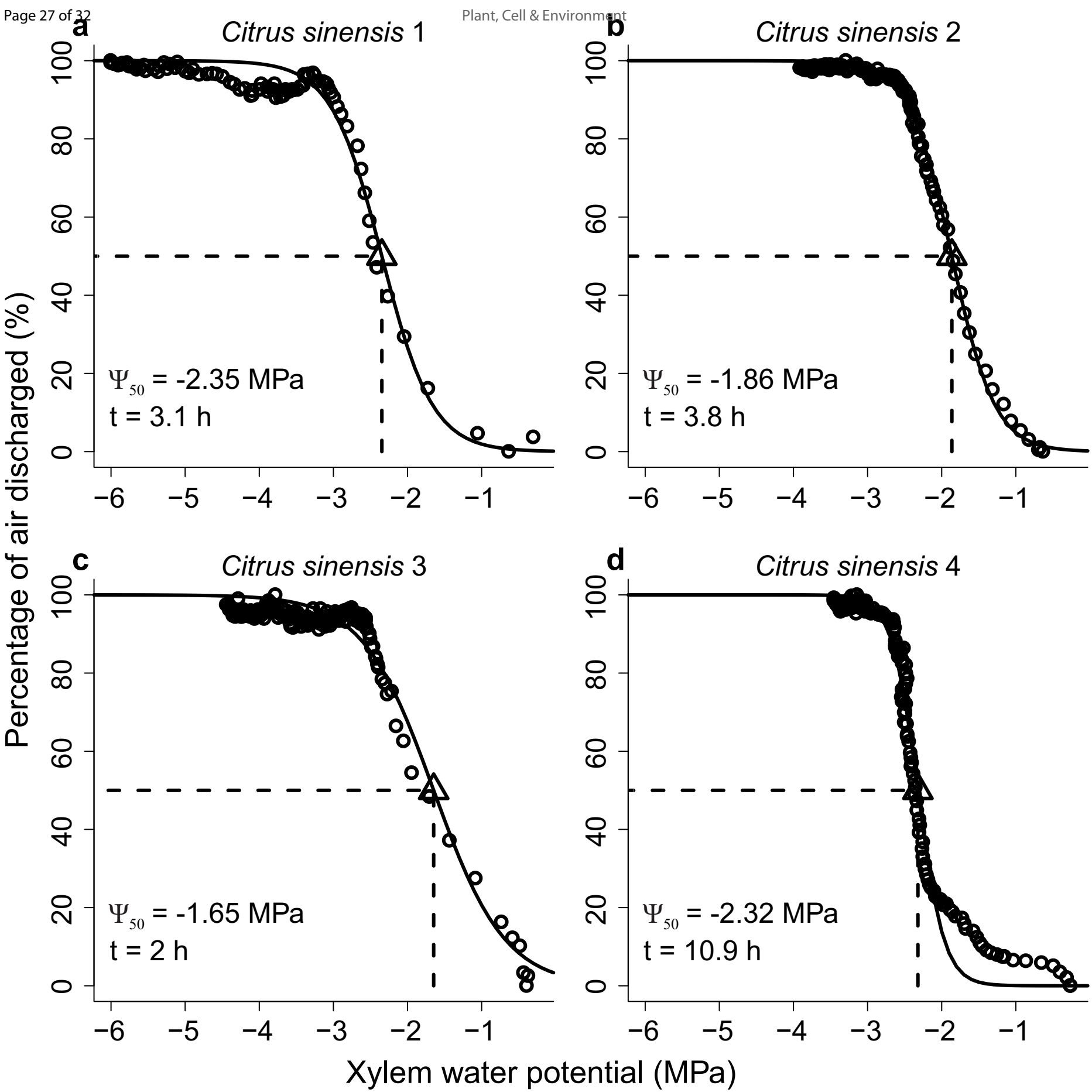
a
Citrus sinensis 1
Ψ50 = -2.35 MPa
t = 3.1 h
b
Citrus sinensis 2
Ψ50 = -1.86 MPa
t = 3.8 h
c
Citrus sinensis 3
Ψ50 = -1.65 MPa
t = 2 h
d
Citrus sinensis 4
Ψ50 = -2.32 MPa
t = 10.9 h
Percentage of air discharged (%)
Xylem water potential (MPa)
0
20
40
60
80
100
−6
−5
−4
−3
−2
−1

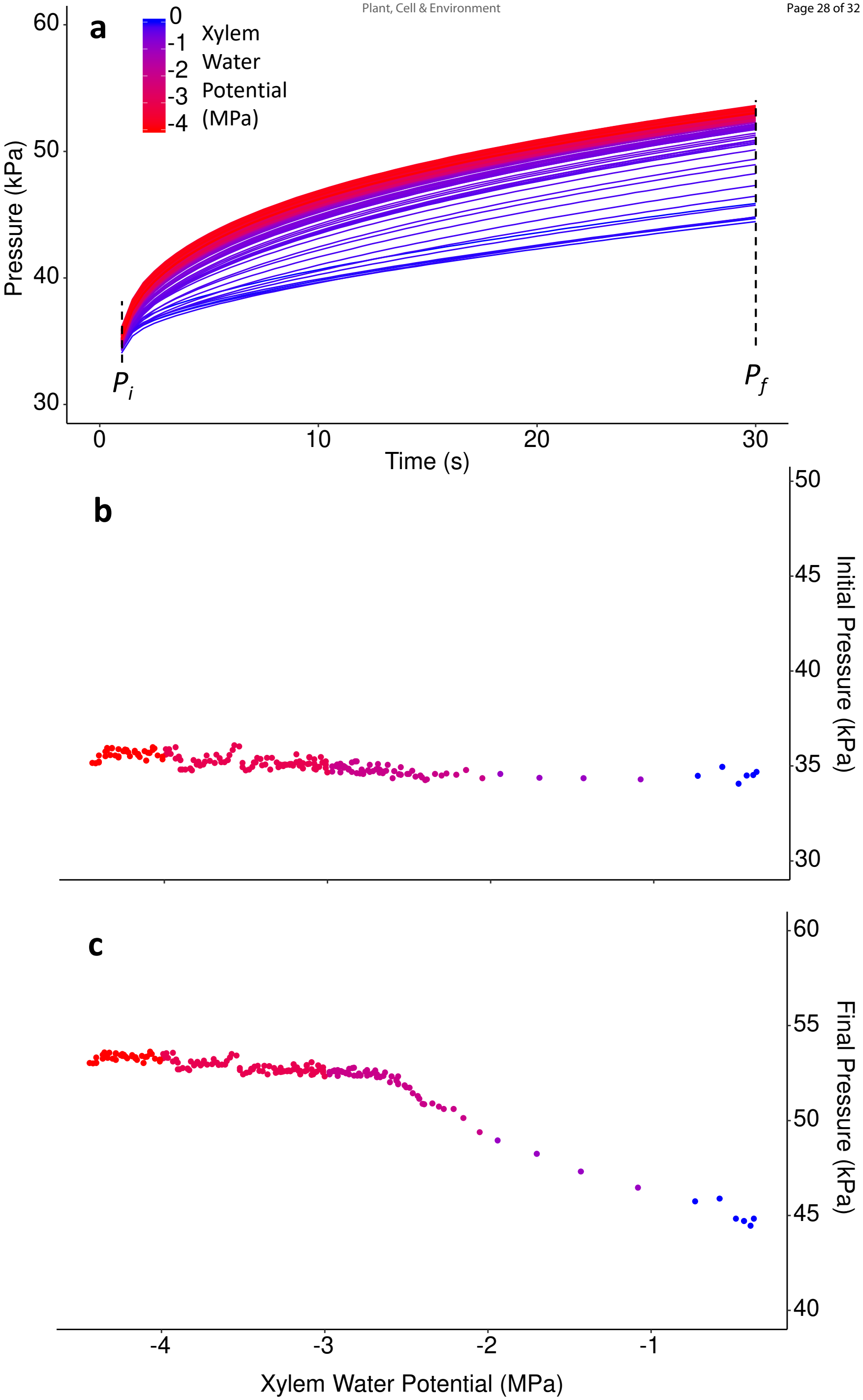
a
0
-1
-2
-3
-4
Xylem
Water
Potential
(MPa)
Pressure (kPa)
60
50
40
30
P_i
P_f
0
10
20
30
Time (s)
b
50
45
40
35
30
Initial Pressure (kPa)
c
60
55
50
45
40
Final Pressure (kPa)
-4
-3
-2
-1
Xylem Water Potential (MPa)

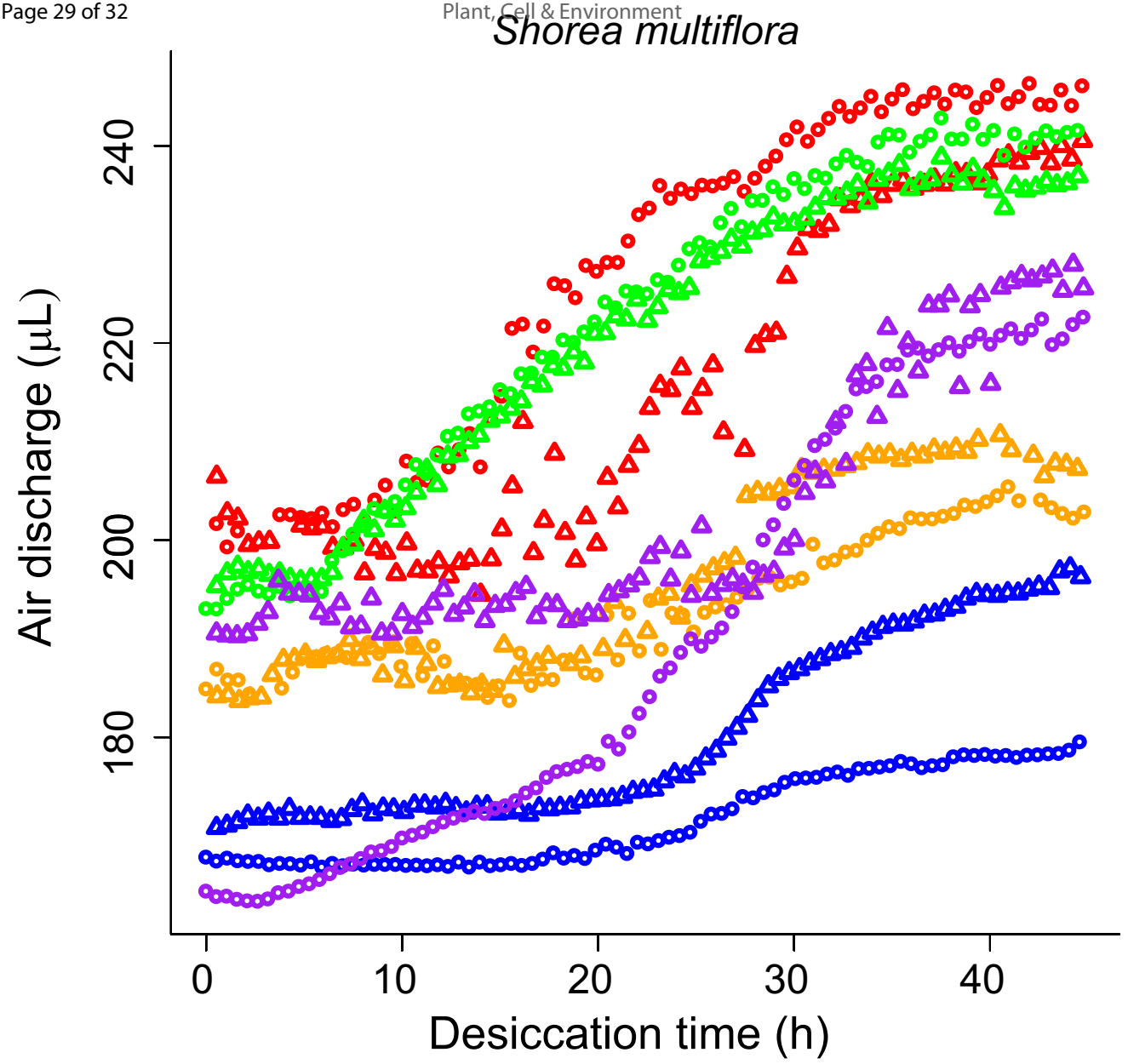
Shorea multiflora
Air discharge (µL)
180
200
220
240
0
10
20
30
40
Desiccation time (h)

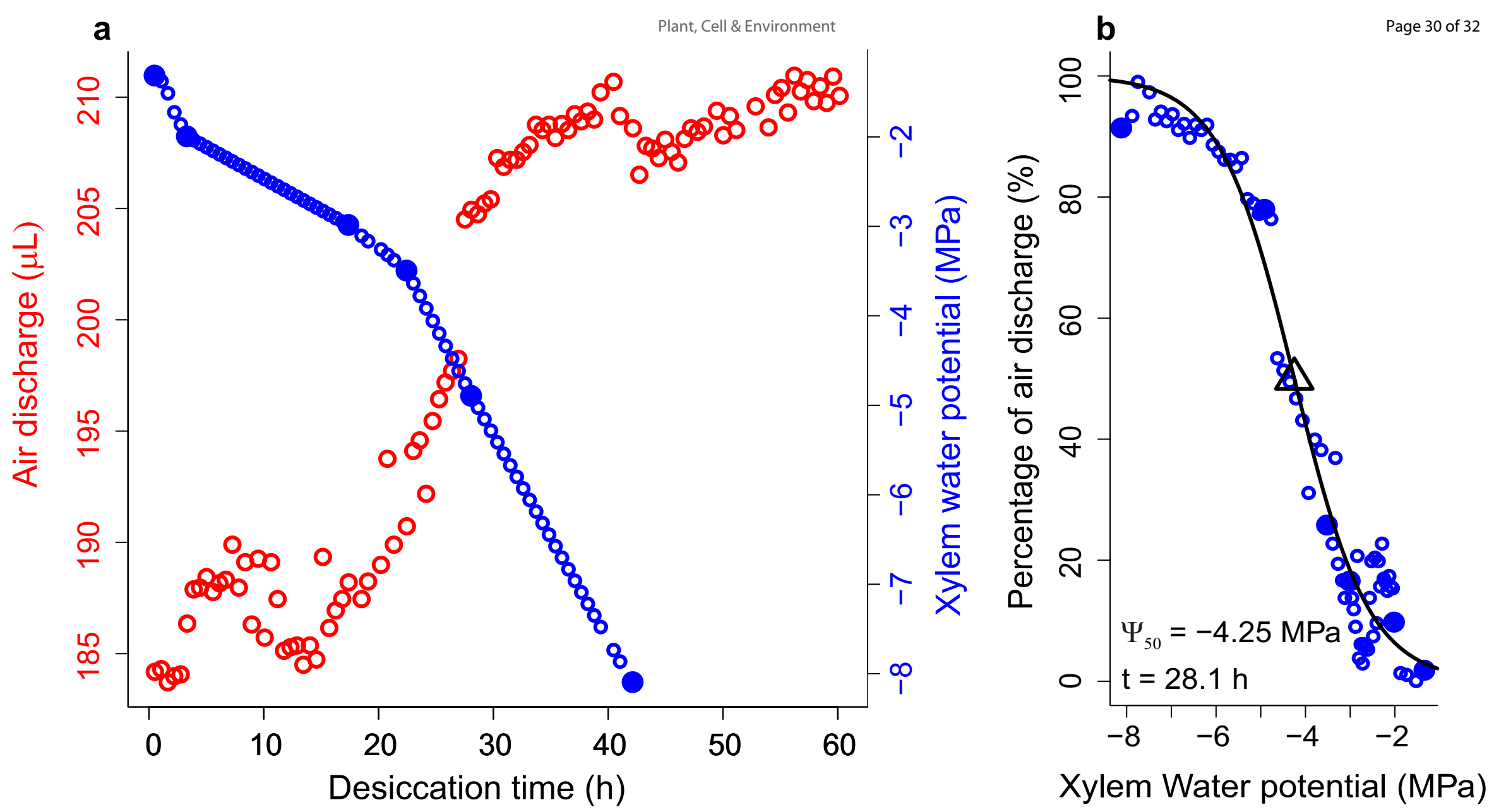
a
Air discharge (µL)
185
190
195
200
205
210
Xylem water potential (MPa)
−2
−3
−4
−5
−6
−7
−8
0
10
20
30
40
50
60
Desiccation time (h)
b
Percentage of air discharge (%)
0
20
40
60
80
100
Ψ50 = −4.25 MPa
t = 28.1 h
−8
−6
−4
−2
Xylem Water potential (MPa)

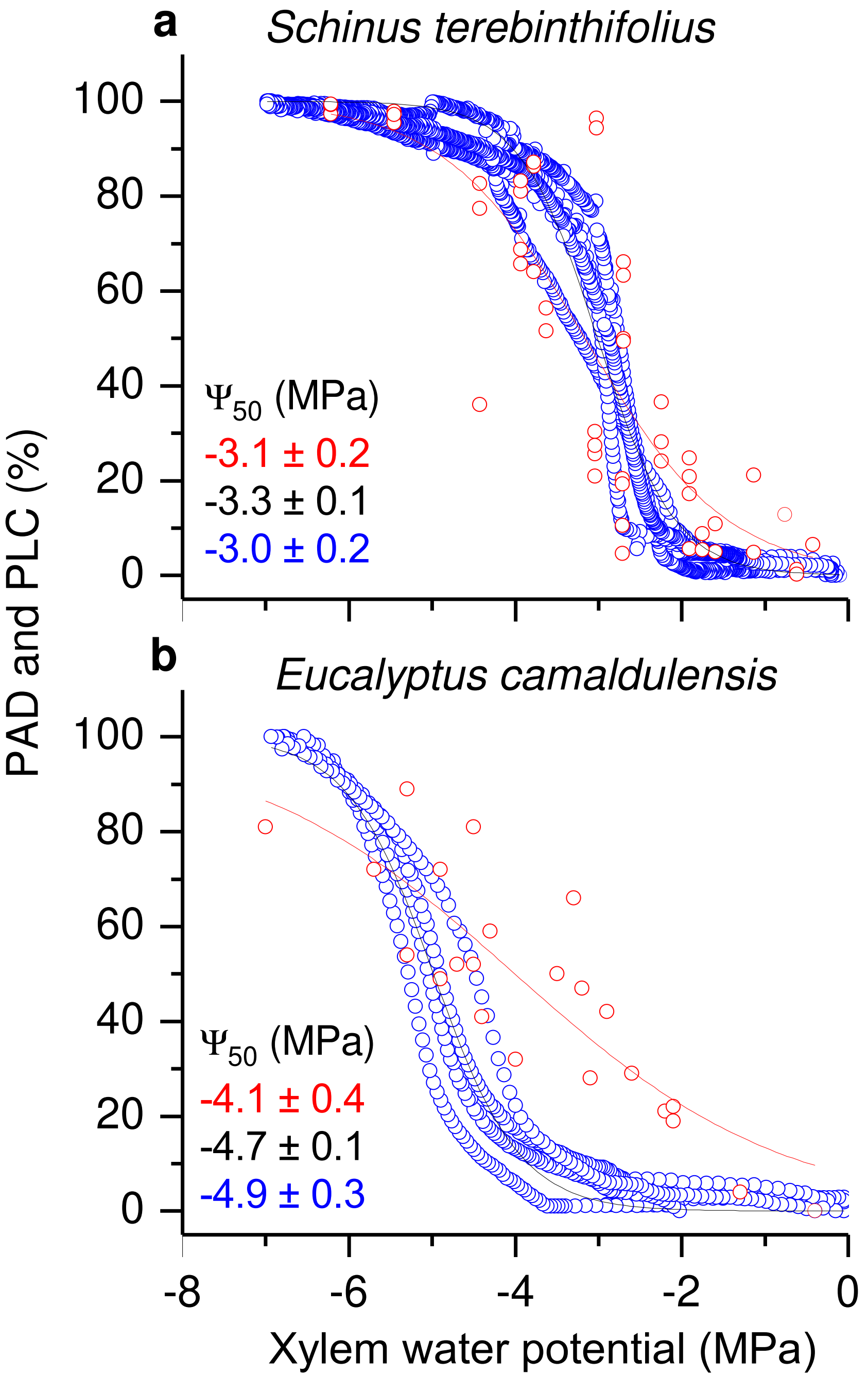
a
Schinus terebinthifolius
100
80
60
40
20
0
PAD and PLC (%)
Ψ50 (MPa)
-3.1 ± 0.2
-3.3 ± 0.1
-3.0 ± 0.2
b
Eucalyptus camaldulensis
100
80
60
40
20
0
Ψ50 (MPa)
-4.1 ± 0.4
-4.7 ± 0.1
-4.9 ± 0.3
-8
-6
-4
-2
0
Xylem water potential (MPa)

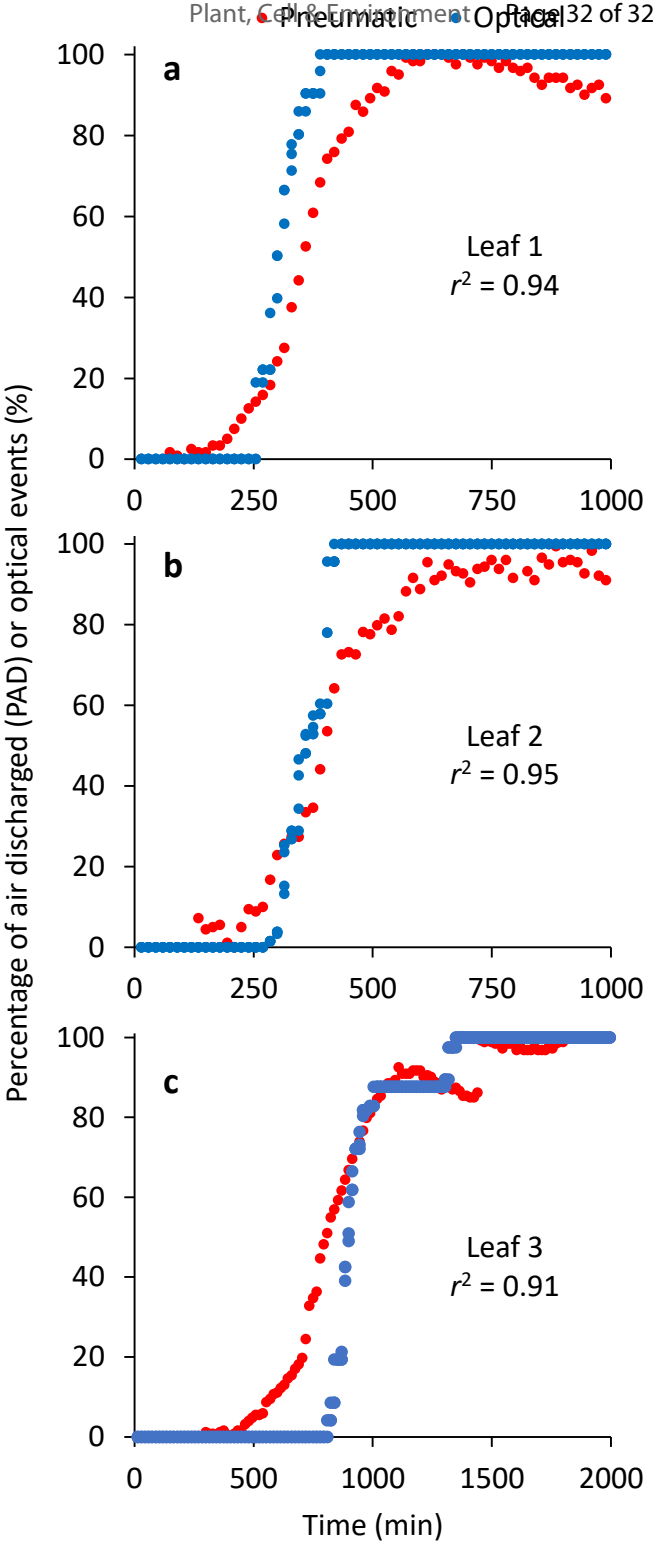
Pneumatic
Optical
a
Leaf 1
r^2 = 0.94
b
Leaf 2
r^2 = 0.95
c
Leaf 3
r^2 = 0.91
Percentage of air discharged (PAD) or optical events (%)
Time (min)
0
20
40
60
80
100
0
250
500
750
1000
1500
2000